

Protein Variants in Cancer-Related Genes

Subjects: Genetics & Heredity | Medicine, Research & Experimental | Oncology

Contributor: Roberta Chiaraluce, Maria Petrosino, Alessandra Pasquo, valerio consalvi

Large scale genome sequencing allowed the identification of a massive number of genetic variations, whose impact on human health is still unknown. In this entry we analyze, by an in silico-based strategy, the impact of missense variants on cancer-related genes, whose effect on protein stability and function was experimentally determined. We collected a set of 164 variants from 11 proteins to analyze the impact of missense mutations at structural and functional levels, and to assess the performance of state-of-the-art methods (FoldX and Meta-SNP) for predicting protein stability change and pathogenicity.

Keywords: protein structure ; protein stability ; protein function ; single amino acid variant ; putative cancer driving variant ; free-energy change

1. Experimental Analysis of Protein Variants in Cancer-Related Genes

The missense variants of our dataset affect tumor suppressor genes, such as BRCA1 [1] and TP53 [2], or proteins involved in the regulation of cell metabolism, such as phosphoglycerate kinase 1 (PGK1) and human frataxin (hFXN) [3] as well as proteins involved in the epigenetic regulation of gene transcription and master transcriptional factors, such as bromodomains (BRDs) [4], protein kinase PIM-1, and Protein tyrosine phosphatase ρ (PTP ρ), whose dysregulation can influence different signaling pathways [5], and peroxisome proliferator receptor γ (PPAR γ), a nuclear receptor involved in several biological processes and in the maintenance of cellular homeostasis [6].

The analysis of the mutation sites in all the protein structures examined indicates that ~30% of them are buried from the solvent. Generally, the consequence of a mutation in the protein core are more likely to be deleterious, leading to protein misfolding [7]. If the mutated residue is on the surface of the protein, a minimal rearrangement of the exposed region may occur, however the global folding of the protein variant is maintained as well as its expression in the cell [8][9]. In either cases, missense mutations can lead to loss of function when generating unstable mutant proteins more susceptible to proteolysis, directly affecting binding affinity [10][11], or protein expression levels [12]. However, destabilizing mutations may also confer new functions when promoting interactions with new partners [13] or aggregation [14].

1.1. Effect on Protein Stability

Stability is a fundamental property of a protein [15][16] and it is one of the protein properties mostly affected by missense mutations [17][18]. About 80% of missense mutations associated with disease result in alteration of protein stability affecting it by several kcal/mol [17]. Therefore, it becomes essential to annotate whether a single nucleotide substitution associated to a given disease generates a SAV with a different stability [19].

Missense mutations may increase the conformation energy of the native state, destabilizing it and making the protein more prone to aggregation [14][20], which is a decisive event in some diseases characterized by aggregates of unfolded proteins [21]. However, in some cases, a mutation decreases the free energy of the native state, which might also turn out to be deleterious, if the increased stability limits the conformational changes important for the functionality of the protein. Generally, most disease-causing mutations are destabilizing [22][23][24]: if a mutation affects a stabilizing interaction within a folded protein, e.g., hydrophobic interactions or a network of hydrogen bonds, the native state may be destabilized. The loss of stability may be accompanied by loss of function [25], since most proteins need to be folded for functioning. The degree of destabilization is elevated for mutations introducing drastic changes, such as charged to neutral, or aromatic to aliphatic residue, that are often related to diseases. A consequence of the decrease in SAVs structural stability may be an increased proteolysis, which may lead to an insufficient amounts of that protein in the cells [26].

Folding studies and stability analysis have been performed on several missense variants of different proteins, measuring, by thermal or chemical unfolding, the impact of single amino acid substitution on the difference in Gibbs free energy value between the mutated and wild-type protein ($\Delta\Delta G_f$). The tumor suppressor p53 is one of the most frequently mutated proteins found in cancer [27][28][29]. Among the selected mutations of p53, many of them distributed throughout the core

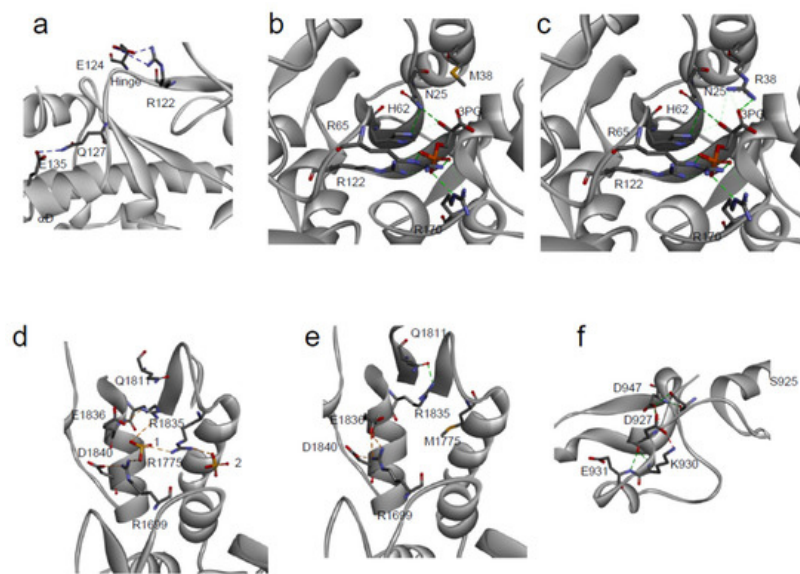


Figure 2. Local environment of SAVs. (a) PIM-1: Detailed view of the local structural environment around the mutated residue E135 [34]; (b,c) PGK1: detail of the 3 phosphoglycerate (3-PG) binding site in the variant p.R38M (b) in comparison with the wild-type (c) [35]; (d,e) BRCA1: Structural rearrangements of p.M1775R variant (d) in comparison with the wild-type, 1 and 2 are two solvent ions (e) [36]; (f) PTPp: local environment of the mutated residue D927 [22].

The minor conformational changes, observed in SAVs by near-UV CD and fluorescence emission, can also be observed as minimal changes in their 3D structure. The crystal structure of PGK1 p.R38M somatic variant [35] is closely similar to that of the corresponding wild-type and only local differences can be detected. The residue R38 is placed in the N-terminal 3-phosphoglycerate binding domain, where it is important for substrate binding, and its correct positioning is required to react with ADP (Figure 3c).

Moreover, together with residues K215 and K219, R38 is critical for charge balancing of the transition state, directly interacting with the transferring phosphate group in the closed conformation of PGK1. Compared to the wild-type structure, the overall structure of p.R38M is conserved (Figure 2g and Figure 3b,c), with only minor differences between the two: at the level of α -helix 374–382, visible in the p.R38M variant but not in the wild-type, and in the position of the β -phosphate group, which in p.R38M points towards the helix (Figure 3b,c).

Despite the minimal changes in the p.R38M crystal structure, a dramatic effect of mutation on the kinetic parameters of PGK1 was observed; K_M increased from 0.40 to 3.15 mM and the turnover number strongly decreased from 89.8 to $7.2 \times 10^{-6} \text{ s}^{-1}$. This confirms that local and minimal changes in the protein structure, induced by a missense mutation, can lead to major alterations in protein function.

The impact of cancer-related missense mutations on protein structure can be dramatic, as demonstrated by the interesting example of the BRCA1 p.M1775R (Figure 3d). BRCA1 is involved in the regulation of multiple nuclear functions, including transcription, recombination, DNA repair, and checkpoint control, and is frequently mutated in cancer [37]. The p.M1775R variant of the C-terminal domain of BRCA1 (BRCT) cannot interact with histone deacetylases [38], the DNA helicase BACH1 [39], or with the transcriptional co-repressor CtIP [40][41]. The residue p.M1775 is largely buried and its substitution with an arginine residue creates a clustering of three positively charged residues (R1699, R1775 and R1835) (Figure 3d,e). In the wild-type native structure, R1699 participates in the sole conserved salt bridge of the inter-BRCT repeat, formed with a pair of carboxyl-terminal BRCT acidic residues, D1840 and E1836 (Figure 3e). R1835 normally participates in a hydrogen bonding network with Q1811, thereby helping to orient the β^1 - α^1 loop (Figure 3c). In the p.M1775R variant, R1699 retains the salt bridge with D1840 but no longer contacts E1836 and instead coordinates an anion, R1835 rotates away from Q1811 and forms a new salt bridge with E1836 (Figure 3d) [32][36].

1.3. Effect on Protein Interactions

Approximately 60% of disease-associated SAVs show significant perturbations in the protein binding sites, resulting in complete loss of interactions and/or function [42][43][44]. In particular, if the mutated residue is essential in contributing to the interactions with partners [45][46][47][48], the binding affinity, as well as the binding specificity, would be dramatically affected, due to geometrical constraints and/or energetic effects [49][50][51][52]. For example, the deleterious mutations E330K and G352R of SMAD4, clustered near the SMAD4–SMAD3 interaction interface, are associated with juvenile polyposis [53][54]. This observation is in agreement with previous evidence associating the juvenile polyposis with the disruption of the signaling pathway TGF β /SMAD which includes the interaction of SMAD4–SMAD3 [55][56].

Several SAVs exhibit alterations in their binding properties. An interesting example is represented by the BRDs, small helical interaction modules that specifically recognize acetylation sites in proteins. BRD2(1) (Figure 2b) and BRD3(2) SAVs show significant differences in their binding to two inhibitors of pharmacological interest, PFI-1 and JQ1, that may be related to the location of the missense mutations in proximity of a region important for the binding to acetylated peptides [57].

1.4. Effect on Protein Catalytic Activity

In the human population, 25% of the known SAVs show a significant modification of their biological function [21]. This percentage is mostly covered by mutations that occur in the active sites of enzymes or in the binding pockets of receptors [58][59]. Biochemical reactions are very sensitive to the precise geometry of the active sites [60][61][62]. Enzyme catalysis, however, does not depend just on a restricted number of crucial residues in the catalytic pocket, but also on several surrounding residues, important for ensuring the proper positioning of the substrates and cofactors into the active site. Therefore, mutations that occur on the residues located in the neighborhood of the active site, although not directly involved in the catalytic event, may also influence the enzyme activity [60][61], as in the case of PGK1 SAVs, discussed in Section 3.2 (Figure 3b). An interesting example of changes in enzyme tyrosine phosphatase activity, due to the presence of missense mutations, is represented by the case of PTPp (Figure 2f), that belongs to the classical receptor type IIB family of protein tyrosine phosphatase and may act as a tumor suppressor [63]. Among the PTPp SAVs identified in human cancer tissues, the missense variant p.D927G is almost completely inactive at 37°C [22]. This mutation involves a solvent exposed residue, distant from the catalytic site, and placed in a 4-residues turn between two coils, that connects different secondary structure regions through hydrogen bonds with three residues (D947, K930, and E931) (Figure 3f). The highly destabilizing D927G mutation may presumably alter the main chain flexibility, leading to local disorder, and thus affecting the stabilizing hydrogen bonds of residues in its proximity [22]. This SAV is an interesting example of the cumulative effect of a missense mutation on thermodynamic stability and function.

2. Computational Analysis of Protein Variants in Cancer-Related Genes

The large amount of protein variants collected in public databases and the limitations in the experimental methods stimulated the development of several tools for predicting their impact on protein stability and their pathogenic effect. Accordingly, early developed tools focus on the prediction of protein stability change by estimating the variation of free energy change ($\Delta\Delta G_f$) resulting from an amino acid substitution [64][65]. The majority of methods, which have been trained on ProTherm database [66] or on manually collected datasets [67], predict either the value or the sign (positive/negative) of the $\Delta\Delta G_f$. More recently, once large databases collecting pathogenic variants were made available, many binary classifiers have been implemented for predicting the impact of genetic variants on human health [68][69][70]. All available methods for predicting the impact of variants on protein stability or on protein pathogenicity rely on the various features extracted from protein sequence, structure, and evolutionary information. State-of-the-art methods of both types are currently used for protein engineering and for variant interpretation. In this section, we analyze the effect of the protein variants using computational approaches for predicting protein stability changes and pathogenicity, with the aim of estimating the role of protein stability on cancer mechanisms and the reliability of computational tools on this specific task.

2.1. Collection of the Protein Variant Datasets

In this work, we analyze a set of 164 missense variants from 11 proteins to understand the contribution of protein stability on the insurgence and progression of cancer. Among the 11 proteins, 5 of them are mainly involved in regulation activities (BRD2, BRD3, BRD4, p16, and PPARy), 4 have catalytic activities (PIM1, PGK1, FXN, and PTPp) while the remaining 2 (p53 and BRCA1) are involved in many biological processes. The set collects all protein variants, for which the folding $\Delta\Delta G_f$ value was experimentally determined and whose genes are reported in the COSMIC database, either as Tier 1 genes, or with putative cancer-driving evidence. The folding $\Delta\Delta G_f$ is calculated as the difference between the folding ΔG of the mutant and wild-type proteins ($\Delta\Delta G_f = \Delta G_f^{mut} - \Delta G_f^{wt}$), i.e., it is positive for destabilizing variants. When available, the variation of the melting temperature ($\Delta T_m = T_m^{mut} - T_m^{wt}$) was also collected. The distributions of the $\Delta\Delta G_f$ and ΔT_m values are plotted in Figure 3a. The protein mutants are mapped on unique protein structures except in the case of p53, for which the DNA binding and oligomerization domains are considered separately. A subset of 97 variants from 9 proteins is obtained by matching our dataset with the data collected by the Cancer Mutation Census (CMC) project. This subset is composed of 24 putative cancer-driving variants annotated as “Tier 1–3” and 63 putative benign variants annotated as “Other”.

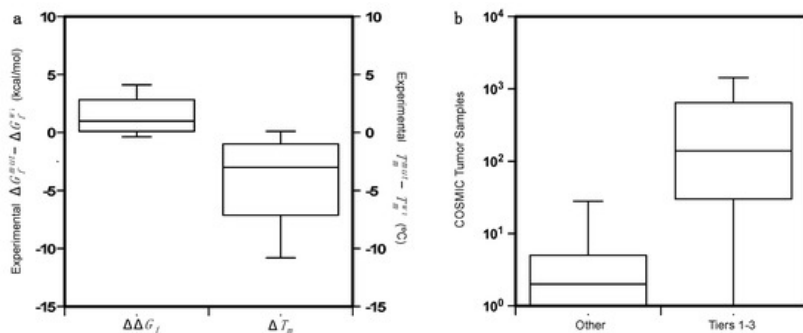


Figure 3. (a) Distributions of the of $\Delta\Delta G_f$ and ΔT_m on the dataset of 164 protein variants. ΔT_m is available only for 73 of them. (b) Comparison of the distributions of the COSMIC tumor samples for the putative cancer-driving variants (Tiers 1–3) and the benign variants (*Others*) annotated by the Cancer Mutation Census project.

In [Figure 4b](#) we compared the distribution of the COSMIC tumor samples in which the putative cancer-driving variants (PCVs) and putative benign variants were detected. The somatic variants annotated by the CMC project are found in different tumor tissues. In particular, the hotspot mutants in the p53 DNA-binding region are detected in tumors from more than 30 tissues.

2.2. Analysis of the Protein Variants

In this review we verified the possibility of using the available methods for predicting the impact of missense variants to identify key functional residues of the protein. We first evaluated the performance of a state-of-the-art method (FoldX [\[71\]](#)) in the prediction of $\Delta\Delta G_f$ resulting from an amino acid substitution. In the second step of the analysis, we predicted the pathogenicity of the selected variants to identify putative cancer-driving variants. For this task we used Meta-SNP [\[72\]](#), a meta prediction algorithm combining the output of 4 methods, namely PhD-SNP [\[73\]](#), PANTHER [\[74\]](#), SIFT [\[75\]](#), and SNAP [\[76\]](#). The Meta-SNP output is considered as a proxy for predicting PCVs as reported in the Cancer Mutation Census (<https://cancer.sanger.ac.uk/cmc> (accessed on 1 May 2021)). For optimizing the prediction process on our set of cancer-associated genes we performed a 5-fold cross-validation procedure to select the best classification threshold. For a better characterization of the results, we also evaluated the importance of protein structure and evolutionary information in the detection of putative cancer-driving variants.

2.3. Predicting the Folding Free Energy Change of the Protein Variants

For each mutant in our dataset, we predicted the variation of the folding free energy ($\Delta\Delta G_f$) using FoldX, which is one of the most accurate methods for such a task [\[24\]](#). For each mutant, we averaged the FoldX predictions on 10 models of the mutated structure. We then compared the predicted and the experimental $\Delta\Delta G_f$ values and calculated the performance on the set of variants, either grouped by proteins or on the whole set. In particular, we calculated three types of correlation (Pearson, Spearman, Kendall-Tau), and two error estimates, the Root Mean Square Error (RMSE) and the Mean Absolute Error (MAE). The results in [Table S2](#) show that, on the whole set of 164 variants, FoldX achieves a Pearson correlation coefficient (r_p) of 0.50 and a RMSE of 2.1 kcal/mol. This result can be improved by removing the variant p.G1788V of BRCA1 from the dataset. For that variant, FoldX predicts a $\Delta\Delta G_f$ of 15.2 kcal/mol, which is much higher than all other predicted values. Such a large predicted $\Delta\Delta G$ value is likely due to a limitation of FoldX, which in this case fails to identify a stable conformation of the protein mutant. After removing p.G1788V from the dataset, the r_p increased to 0.56 and the RMSE decreased to 1.8 kcal/mol. On average we observed that the predicted $\Delta\Delta G$ values returned by FoldX tend to be larger than the experimental values. This behavior is probably due to the implementation of the FoldX algorithm which predicts the structure of the mutant protein only considering different rotamers of the amino acid side chains. Such a process might limit the ability of the tool to identify more stable conformations that could be obtained through the rearrangement of the backbone.

Further analysis was performed after grouping the variants by proteins and calculating the performance on the resulting protein subsets. By doing so, we observed for some proteins (both domains of p53, hFXN, PGK1, and PTPp) a $r_p > 0.58$. For other proteins (BRDs, PIM-1, and p16) with a smaller number of mutants (≤ 10), we observed lower or negative correlation coefficients. The scatter plots, showing the correlation between predicted and experimental $\Delta\Delta G_f$ values for the whole set of proteins, or for the proteins with the highest number of mutants (p53 and BRCA1), are shown in [Figure 4](#). Another interesting analysis consists in the prediction of highly destabilizing variants ($\Delta\Delta G_f > 2$ kcal/mol). In this case, we have used FoldX as a binary classifier, optimizing a threshold on its output.

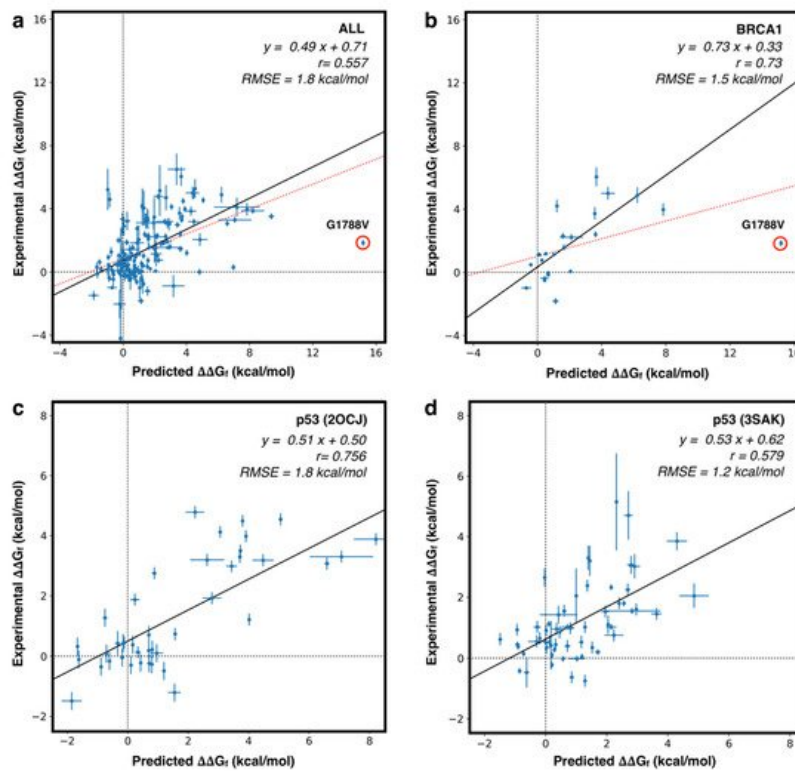


Figure 4. Scatter plot for predicted vs experimental $\Delta\Delta G_f$ values. **(a)** fitting on the whole set of 164 variants (red) and after removing the outlier BRCA1 p.G1788V (black). **(b)** Similar analysis performed on the whole set of variants in BRCA1 (red) and after removing BRCA1 p.G1788V variant (black). **(c,d)** fitting on the subset of variants in p53 core (2OCJ) and oligomeric (3SAK) domains, respectively. r : Pearson correlation coefficient. RMSE: Root Mean Square Error.

The optimization procedure, based on balancing the true positive and true negative rates, shows that FoldX can achieve an overall accuracy of 77% and a Matthews Correlation Coefficient (MCC) of 0.55 when a prediction threshold of ~ 1.2 kcal/mol is considered for the whole set of 164 variants. This method shows a good performance also when considering protein-specific thresholds. Indeed, for the subset of proteins with the highest number of mutants (p53 and BRCA1), the performance in the classification task reached MCC = 0.78 and AUC (Area Under the ROC curve) = 0.95 for the DNA binding domain of p53, or MCC = 0.67 and AUC = 0.90 for BRCA1. All performance measures in the classification task are summarized in [Table S3](#).

In general, our analysis confirms that, on average, the predicted and experimental $\Delta\Delta G_f$ correlate well, and that the FoldX prediction can be used to estimate the impact of mutations of protein stability, in spite of the fact that the prediction error still remains ~ 2.0 kcal/mol. To partially address this limitation, the methods for $\Delta\Delta G_f$ prediction can be used as binary classifiers to detect highly destabilizing protein variants.

2.4. Predicting the Pathogenicity of Protein Variants

In the last decade, several methods have been developed for predicting the pathogenicity of variants. In general, those approaches are binary classifiers, based on the analysis of evolutionary conservation. The idea behind these tools is based on the observation that mutations occurring in highly conserved regions of the protein are more likely to be pathogenic than mutations in variable regions. In the case of cancer-associated variants, the validation of the predictive methods is a difficult task due to the lack of curated sets of annotated variants. To address this issue, the COSMIC curators are annotating the somatic mutations in the Cancer Mutation Census (CMC) dataset [22]. Currently, the CMC contains ~ 3 million missense variants, only $\sim 0.1\%$ of which were curated. Using such annotation, we analyzed the prediction of Meta-SNP, an algorithm combining the output of 4 methods, on our dataset. Initially, we analyzed the relationship between the experimental $\Delta\Delta G_f$ and the variant pathogenicity score returned by Meta-SNP, to test its performance in the detection of highly destabilizing variants ($\Delta\Delta G_f > 2$ kcal/mol). Setting the optimized classification threshold to 0.66, we found that Meta-SNP reaches an accuracy of 73% and a Pearson correlation coefficient of 0.40 in the classification of highly destabilizing variants. We also estimated the performance of Meta-SNP in the prediction of putative cancer-driving variants (PCVs), assuming that missense variants, annotated as “Other” in the CMC database, can be classified as benign and variants in CMC annotated as classes 1–3 (Tier 1–3) can be considered putative cancer-driving variants (PCVs). For a more stringent test we calculated the performance of Meta-SNP by removing from the

dataset 15 mutations used for the training of the method. Our results show that, for the subset of 82 variants annotated in CMC, by using a classification threshold of 0.71, Meta-SNP is able to predict PCVs with 77% accuracy and a Matthews correlation coefficient of 0.37.

The high fraction of false positives in the prediction of highly destabilizing variants may indicate the presence of pathogenicity mechanisms alternative to the loss of stability, while the high rate of false positives in the prediction of PCVs can be due to incorrect and/or incomplete protein variants annotation.

Although the Meta-SNP predictions result in a high fraction of false positive, the PCVs, annotated with 1 to 3 in the CMC database, are enriched in the variants with folding $\Delta\Delta G_f > 2$ kcal/mol with respect to the subset of CMC variant annotated as "Other". Indeed, the relative p-value calculated by the Fisher test is < 0.03 .

Furthermore, the comparison of the distributions of the Meta-SNP output for Tier 1–3 and "Other" variants reveals a significant difference. The average values of the distributions of Meta-SNP outputs for Tier 1–3 and "Other" variants are 0.71 and 0.47, respectively. This difference is statistically significant, corresponding to a Kolmogorov-Smirnov p -value $< 10^{-4}$.

Finally, we also tested the performance of FoldX in predicting PCVs. Our analysis revealed that, selecting a predicted $\Delta\Delta G_f$ threshold of 2.7 kcal/mol, FoldX is able to identify Tier 1–3 variants with 73% overall accuracy and a Matthews correlation coefficient of 0.33. The comparison of the results shows that a predictor of putative pathogenic variants (Meta-SNP) is performing better than a method designed to predict folding $\Delta\Delta G_f$ (FoldX) in the detection of PCVs.

2.5. Analysis of the Prediction on the Basis of the Amino Acid Accessibility and Conservation

In the previous sections, we have shown that protein stability of cancer-related genes can be predicted with a good level of confidence using dedicated computational tools like FoldX. We have also observed that the pathogenicity score, calculated through a consensus method, correlates with protein stability data and with phenotypic data. Nevertheless, the prediction of PCVs, starting from protein stability predictions, is a more complex task. To this end, more experimental data on the stability of cancer proteins and their variants, and a higher level of curation of the existing databases on cancer protein variants would be needed. As an in-silico alternative for estimating the impact of protein variants on the stability and phenotypic levels, we used Meta-SNP, which is one of the state-of-the-art methods that best predict the protein variant pathogenic potential. To better analyze the results obtained by Meta-SNP, we calculated the distributions of solvent accessibility and conservation scores of the wild-type residues for the subset of highly destabilizing and PCVs.

In detail, for each mutated site we calculated the relative solvent accessibility (RSA) of the mutated residues and the frequency of the wild-type residue in the multiple sequence alignment (f_{WT}) of possible homologs of the mutated protein.

As described in [supplementary materials](#), the RSA was calculated by normalizing the solvent accessibility calculated with the DSSP program ^[78] and the f_{WT} was returned as part of the output of the Meta-SNP server (<http://snps.biofold.org/meta-snp>, accessed on 1 May 2021). In the first part of our analysis, we compared the RSA values for the subset of highly destabilizing variants ($\Delta\Delta G > 2.0$ kcal/mol) and the remaining ones, showing that for $RSA \leq 0.2$ there is little overlap between the two distributions ([Figure 5a](#)). In the same range of RSA ([Figure 5b](#)), the PCVs (Tiers 1–3) can be easily discriminated from benign ones ("Other"). In both cases, using the Kolmogorov-Smirnov test to estimate the statistical difference between the two subsets in Figs. 6a and 6b, we obtained p -values $< 10^{-3}$. In particular, [Figure 5b](#) shows that the majority of PCVs (~58%) are occurring in buried regions ($RSA \leq 0.2$), while ~75% of putative benign variants are in exposed regions ($RSA > 0.2$). The fraction of PCVs in exposed regions, which we found in our dataset, is higher than the value reported for pathogenic variants ^[7], nevertheless, due to the reduced size of our dataset, such a difference is not statistically significant.

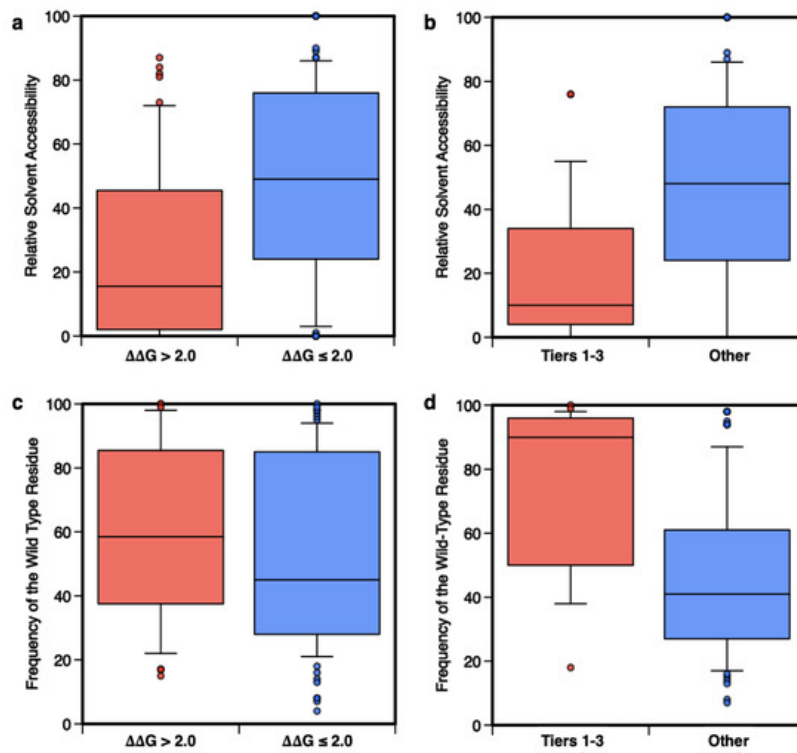


Figure 5. Distributions of the Relative Solvent Accessibility (RSA) and frequency of the wild-type residue (f_{WT}) in the multiple sequences of homolog proteins. The distributions of RSA and f_{WT} calculated for the subsets of 53 highly destabilizing variants ($\Delta\Delta G_f > 2.0$ kcal/mol) compared to the remaining 111 variants ($\Delta\Delta G_f \leq 2.0$ kcal/mol) are shown in panels (a,c). In panels (b,d) the same distributions are plotted for the subsets of 24 putative cancer-driving (Tier 1–3) or 73 benign (‘Other’) variants.

In the second part of this analysis, different results are observed when the distributions of f_{WT} are compared. [Figure 5c](#) shows that conservation is not a strong feature for the classification of highly destabilizing variants, while it is essential for the prediction of PCVs. Indeed, for $f_{WT} > 50\%$ the distributions of Tier 1–3 and ‘Other’ variants have little overlap ([Figure 5d](#)). The comparison between the results in [Figure 5c,d](#) indicates that destabilization and conservation may indeed serve the pathogenicity prediction task as reciprocally integrating features [25].

A further interesting analysis can be performed by considering the distribution in two dimensions of the RSA and f_{WT} together for Tiers 1–3 and ‘Other’ variants. In [Figure 6a](#) we observed an enrichment for Tiers 1–3 variants in the buried (RSA < 20%) and conserved residues ($f_{WT} > 50\%$), with a corresponding p-value of 3×10^{-6} , obtained by considering a binomial distribution with a success probability of 0.247. On the opposite side of the plot (RSA $\geq 20\%$ and $f_{WT} \leq 50\%$), we observed a depletion of PCVs (p-value = 0.02). Finally, we performed a similar analysis by combining the experimental $\Delta\Delta G_f$ with the Meta-SNP predictions ([Figure 6b](#)).

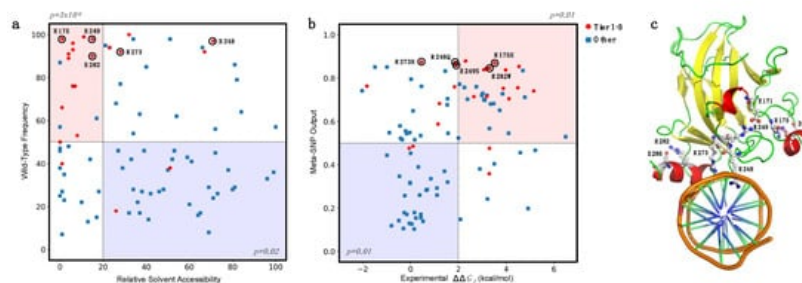


Figure 6. Enrichment and depletion of putative cancer-driving variants (Tier 1–3) in different subgroups. (a) Enrichment of Tier 1–3 variants in mutated sites with Relative Solvent Accessibility $\leq 20\%$ and frequency of the wild-type residue $> 50\%$ (light red). (b) Enrichment of Tier 1–3 variants in the subset of mutants with experimental $\Delta\Delta G_f > 2.0$ kcal/mol and Meta-SNP output > 0.5 (light red). In both cases, the opposite regions (light blue) are depleted of Tier 1–3 variants. In (a,b), the hotspot mutants R175, R248, R249, R273, and R282 are highlighted with black circles. (c) Hotspot sites in the p53 structure in interaction with DNA (PDB:1TUP). Residues R248 and R273 interact with DNA. Residues R175, R249, and R282 are likely to stabilize the protein structure by forming salt bridge interactions with D162, E171, and E286, respectively.

If we considered the subset of highly destabilizing ($\Delta\Delta G_f > 2.0$ kcal/mol) and predicted pathogenic (Meta-SNP output > 0.5) variants, we found an enrichment in Tier 1–3 variants with corresponding p -value of 0.01. On the opposite side of the plot, we observed a depletion of Tier 1–3 variants, again with a p -value of 0.01.

These observations confirm the hypothesis that relative solvent accessibility and amino acid conservation are important features for predicting the impact of amino acid substitution in terms of protein stability and pathogenicity. Furthermore, the combination of the experimental $\Delta\Delta G_f$ and the predicted pathogenicity of variants allows to select a subset of variants with a significantly high probability of having a deleterious phenotypic effect.

In particular, focusing on a subset of five hotspot sites of p53 [79][80], we observed that R248 and R273 are directly interacting with the DNA, in agreement with their high RSA, while R175, R249, and R282 (low RSA) are surrounding the DNA binding site (Figure 7c). These structural aspects, combined with our predictions, support the hypothesis that the p.R248Q and p.R273H variants (with high pathogenicity score but low $\Delta\Delta G_f$) have a direct impact on the protein function of DNA-interaction, while p.R175H and p.R282W (with both high pathogenicity score and high $\Delta\Delta G_f$) destabilize the p53 structure. An intermediate case is p.R249S, which shows a variation of folding free energy of ~ 2 kcal/mol and a low RSA. Similar to R175 and R282, the presence of an oppositely charged residue (E171) in the proximity of R249 suggests that a mutation in this site can indeed reduce the stability of p53, due to a missing salt bridge interaction. Although a significant difference between predicted and experimental $\Delta\Delta G_f$ values (RMSE = 3.2 kcal/mol) is observed for the five hotspots, similar results are obtained when combining the Meta-SNP output with the predicted $\Delta\Delta G_f$ (Figure S1). Our analysis can be compared with the experimental data on DNA-binding affinity of the p53 mutants [30]. The data show that among the five hotspots cancer mutants shown in Figure 7, the three of them with low impact on p53 stability (p.R248Q, p.R249S, and p.R273H with $\Delta\Delta G_f \leq 2.0$ kcal/mol) had no detectable binding affinity with the gadd45 promoter DNA (0% with respect to the wild type). This observation supports the hypothesis that protein–DNA interactions may play an important role in the cancer-inducing mechanism of the mutated p53. By analogy, a similar case of compromised protein–DNA or protein–protein interactions might turn out to hold for other cancer-associated mutants, which might not be in the ‘highly destabilizing’ category. The above observation is also in agreement with the possible roles hotspots cancer p53 mutants are considered to play as gain-of-function effectors [79][80], not only for the ‘contact’ mutants p.R248Q and p.R273H, but also for the ‘conformational’ mutants p.R175H, p.R249S, and p.R282W, since an altered p53 binding energy landscape can shift the mutated cells to different functionalities. Furthermore, the data shown in Figure 7 are consistent with the fact that also destabilizing variants can have gain-of-function characteristics, possibly through altered protein–protein interactions [3].

References

1. Miki, Y.; Swensen, J.; Shattuck-Eidens, D.; Futreal, P.A.; Harshman, K.; Tavtigian, S.; Liu, Q.; Cochran, C.; Bennett, L. M.; Ding, W. A Strong Candidate for the Breast and Ovarian Cancer Susceptibility Gene BRCA1. *Science* 1994, 266, 66–71.
2. Kandoth, C.; McLellan, M.D.; Vandin, F.; Ye, K.; Niu, B.; Lu, C.; Xie, M.; Zhang, Q.; McMichael, J.F.; Wyczalkowski, M. A.; et al. Mutational Landscape and Significance across 12 Major Cancer Types. *Nature* 2013, 502, 333–339.
3. Guccini, I.; Serio, D.; Condò, I.; Rufini, A.; Tomassini, B.; Mangiola, A.; Maira, G.; Anile, C.; Fina, D.; Pallone, F.; et al. F raxin Participates to the Hypoxia-Induced Response in Tumors. *Cell Death Dis.* 2011, 2, e123.
4. Filippakopoulos, P.; Knapp, S. Targeting Bromodomains: Epigenetic Readers of Lysine Acetylation. *Nat. Rev. Drug Discov.* 2014, 13, 337–356.
5. Ruvolo, P.P. Role of Protein Phosphatases in the Cancer Microenvironment. *Biochim. Biophys. Acta Mol. Cell Res.* 2019, 1866, 144–152.
6. Sauer, S. Ligands for the Nuclear Peroxisome Proliferator-Activated Receptor Gamma. *Trends Pharmacol. Sci.* 2015, 36, 688–704.
7. Savojardo, C.; Manfredi, M.; Martelli, P.L.; Casadio, R. Solvent Accessibility of Residues Undergoing Pathogenic Variations in Humans: From Protein Structures to Protein Sequences. *Front. Mol. Biosci.* 2021, 7.
8. Gilis, D.; Rooman, M. Stability Changes upon Mutation of Solvent-Accessible Residues in Proteins Evaluated by Database-Derived Potentials. *J. Mol. Biol.* 1996, 257, 1112–1126.
9. Wei, Q.; Xu, Q.; Dunbrack, R.L. Prediction of Phenotypes of Missense Mutations in Human Proteins from Biological Assemblies. *Proteins* 2013, 81, 199–213.
10. Duning, K.; Wennmann, D.O.; Bokemeyer, A.; Reissner, C.; Wersching, H.; Thomas, C.; Buschert, J.; Guske, K.; Franke, V.; Flöel, A.; et al. Common Exonic Missense Variants in the C2 Domain of the Human KIBRA Protein Modify Lipid

Binding and Cognitive Performance. *Transl. Psychiatry* 2013, 3, e272.

11. Feinberg, H.; Rowntree, T.J.W.; Tan, S.L.W.; Drickamer, K.; Weis, W.I.; Taylor, M.E. Common Polymorphisms in Human Langerin Change Specificity for Glycan Ligands. *J. Biol. Chem.* 2013, 288, 36762–36771.
12. Haraksingh, R.R.; Snyder, M.P. Impacts of Variation in the Human Genome on Gene Regulation. *J. Mol. Biol.* 2013, 425, 3970–3977.
13. Stein, Y.; Rotter, V.; Aloni-Grinstein, R. Gain-of-Function Mutant P53: All the Roads Lead to Tumorigenesis. *Int. J. Mol. Sci.* 2019, 20, 6197.
14. Silva, J.L.; De Moura Gallo, C.V.; Costa, D.C.F.; Rangel, L.P. Prion-like Aggregation of Mutant P53 in Cancer. *Trends Biochem. Sci.* 2014, 39, 260–267.
15. Capriotti, E.; Fariselli, P.; Casadio, R. I-Mutant2.0: Predicting Stability Changes upon Mutation from the Protein Sequence or Structure. *Nucleic Acids Res.* 2005, 33, W306–W310.
16. Zhang, Z.; Wang, L.; Gao, Y.; Zhang, J.; Zhenirovskyy, M.; Alexov, E. Predicting Folding Free Energy Changes upon Single Point Mutations. *Bioinforma. Oxf. Engl.* 2012, 28, 664–671.
17. Wang, Z.; Moulton, J. SNPs, Protein Structure, and Disease. *Hum. Mutat.* 2001, 17, 263–270.
18. Yue, P.; Li, Z.; Moulton, J. Loss of Protein Structure Stability as a Major Causative Factor in Monogenic Disease. *J. Mol. Biol.* 2005, 353, 459–473.
19. Martelli, P.L.; Fariselli, P.; Savojardo, C.; Babbi, G.; Aggazio, F.; Casadio, R. Large Scale Analysis of Protein Stability in OMIM Disease Related Human Protein Variants. *BMC Genom.* 2016, 17 (Suppl. S2), 397.
20. Soragni, A.; Janzen, D.M.; Johnson, L.M.; Lindgren, A.G.; Thai-Quynh Nguyen, A.; Tiourin, E.; Soriaga, A.B.; Lu, J.; Jiang, L.; Faull, K.F.; et al. A Designed Inhibitor of P53 Aggregation Rescues P53 Tumor Suppression in Ovarian Carcinomas. *Cancer Cell* 2016, 29, 90–103.
21. Yue, P.; Moulton, J. Identification and Analysis of Deleterious Human SNPs. *J. Mol. Biol.* 2006, 356, 1263–1274.
22. Pasquo, A.; Consalvi, V.; Knapp, S.; Alfano, I.; Ardini, M.; Stefanini, S.; Chiaraluce, R. Structural Stability of Human Protein Tyrosine Phosphatase ρ Catalytic Domain: Effect of Point Mutations. *PLoS ONE* 2012, 7, e32555.
23. Grothe, H.L.; Little, M.R.; Sjogren, P.P.; Chang, A.A.; Nelson, E.F.; Yuan, C. Altered Protein Conformation and Lower Stability of the Dystrophic Transforming Growth Factor Beta-Induced Protein Mutants. *Mol. Vis.* 2013, 19, 593–603.
24. Khan, S.; Vihinen, M. Performance of Protein Stability Predictors. *Hum. Mutat.* 2010, 31, 675–684.
25. Stein, A.; Fowler, D.M.; Hartmann-Petersen, R.; Lindorff-Larsen, K. Biophysical and Mechanistic Models for Disease-Causing Protein Variants. *Trends Biochem. Sci.* 2019, 44, 575–588.
26. Waters, P.J. Degradation of Mutant Proteins, Underlying “Loss of Function” Phenotypes, Plays a Major Role in Genetic Disease. *Curr. Issues Mol. Biol.* 2001, 3, 57–65.
27. Bykov, V.J.N.; Eriksson, S.E.; Bianchi, J.; Wiman, K.G. Targeting Mutant P53 for Efficient Cancer Therapy. *Nat. Rev. Cancer* 2018, 18, 89–102.
28. Chen, S.; Wu, J.-L.; Liang, Y.; Tang, Y.-G.; Song, H.-X.; Wu, L.-L.; Xing, Y.-F.; Yan, N.; Li, Y.-T.; Wang, Z.-Y.; et al. Arsenic Trioxide Rescues Structural P53 Mutations through a Cryptic Allosteric Site. *Cancer Cell* 2021, 39, 225–239.e8.
29. Gummlich, L. ATO Stabilizes Structural P53 Mutants. *Nat. Rev. Cancer* 2021, 21, 141.
30. Bullock, A.N.; Henckel, J.; Fersht, A.R. Quantitative Analysis of Residual Folding and DNA Binding in Mutant P53 Core Domain: Definition of Mutant States for Rescue in Cancer Therapy. *Oncogene* 2000, 19, 1245–1256.
31. Williams, R.S.; Chasman, D.I.; Hau, D.D.; Hui, B.; Lau, A.Y.; Glover, J.N.M. Detection of Protein Folding Defects Caused by BRCA1-BRCT Truncation and Missense Mutations. *J. Biol. Chem.* 2003, 278, 53007–53016.
32. Rowling, P.J.E.; Cook, R.; Itzhaki, L.S. Toward Classification of BRCA1 Missense Variants Using a Biophysical Approach. *J. Biol. Chem.* 2010, 285, 20080–20087.
33. Petrosino, M.; Pasquo, A.; Novak, L.; Toto, A.; Gianni, S.; Mantuano, E.; Veneziano, L.; Minicozzi, V.; Pastore, A.; Puglisi, R.; et al. Characterization of Human Frataxin Missense Variants in Cancer Tissues. *Hum. Mutat.* 2019, 40, 1400–1413.
34. Lori, C.; Lantella, A.; Pasquo, A.; Alexander, L.T.; Knapp, S.; Chiaraluce, R.; Consalvi, V. Effect of Single Amino Acid Substitution Observed in Cancer on Pim-1 Kinase Thermodynamic Stability and Structure. *PLoS ONE* 2013, 8, e64824.
35. Fiorillo, A.; Petrosino, M.; Ilari, A.; Pasquo, A.; Cipollone, A.; Maggi, M.; Chiaraluce, R.; Consalvi, V. The Phosphoglycerate Kinase 1 Variants Found in Carcinoma Cells Display Different Catalytic Activity and Conformational Stability Compared to the Native Enzyme. *PLoS ONE* 2018, 13, e0199191.

36. Williams, R.S.; Glover, J.N.M. Structural Consequences of a Cancer-Causing BRCA1-BRCT Missense Mutation. *J. Biol. Chem.* 2003, 278, 2630–2635.
37. Venkitaraman, A.R. Cancer Susceptibility and the Functions of BRCA1 and BRCA2. *Cell* 2002, 108, 171–182.
38. Yarden, R.I.; Brody, L.C. BRCA1 Interacts with Components of the Histone Deacetylase Complex. *Proc. Natl. Acad. Sci. USA* 1999, 96, 4983–4988.
39. Cantor, S.B.; Bell, D.W.; Ganesan, S.; Kass, E.M.; Drapkin, R.; Grossman, S.; Wahrer, D.C.; Sgroi, D.C.; Lane, W.S.; Haber, D.A.; et al. BACH1, a Novel Helicase-like Protein, Interacts Directly with BRCA1 and Contributes to Its DNA Repair Function. *Cell* 2001, 105, 149–160.
40. Yu, X.; Wu, L.C.; Bowcock, A.M.; Aronheim, A.; Baer, R. The C-Terminal (BRCT) Domains of BRCA1 Interact in Vivo with CtIP, a Protein Implicated in the CtBP Pathway of Transcriptional Repression. *J. Biol. Chem.* 1998, 273, 25388–25392.
41. Li, S.; Chen, P.L.; Subramanian, T.; Chinnadurai, G.; Tomlinson, G.; Osborne, C.K.; Sharp, Z.D.; Lee, W.H. Binding of CtIP to the BRCT Repeats of BRCA1 Involved in the Transcription Regulation of P21 Is Disrupted upon DNA Damage. *J. Biol. Chem.* 1999, 274, 11334–11338.
42. Schuster-Böckler, B.; Bateman, A. Protein Interactions in Human Genetic Diseases. *Genome Biol.* 2008, 9, R9.
43. Teng, S.; Madej, T.; Panchenko, A.; Alexov, E. Modeling Effects of Human Single Nucleotide Polymorphisms on Protein-Protein Interactions. *Biophys. J.* 2009, 96, 2178–2188.
44. David, A.; Sternberg, M.J.E. The Contribution of Missense Mutations in Core and Rim Residues of Protein-Protein Interfaces to Human Disease. *J. Mol. Biol.* 2015, 427, 2886–2898.
45. Dixit, A.; Verkhivker, G.M. Hierarchical Modeling of Activation Mechanisms in the ABL and EGFR Kinase Domains: Thermodynamic and Mechanistic Catalysts of Kinase Activation by Cancer Mutations. *PLoS Comput. Biol.* 2009, 5, e1000487.
46. Dixit, A.; Yi, L.; Gowthaman, R.; Torkamani, A.; Schork, N.J.; Verkhivker, G.M. Sequence and Structure Signatures of Cancer Mutation Hotspots in Protein Kinases. *PLoS ONE* 2009, 4, e7485.
47. Dixit, A.; Torkamani, A.; Schork, N.J.; Verkhivker, G. Computational Modeling of Structurally Conserved Cancer Mutations in the RET and MET Kinases: The Impact on Protein Structure, Dynamics, and Stability. *Biophys. J.* 2009, 96, 858–874.
48. Acuner Ozbabacan, S.E.; Gursoy, A.; Keskin, O.; Nussinov, R. Conformational Ensembles, Signal Transduction and Residue Hot Spots: Application to Drug Discovery. *Curr. Opin. Drug Discov. Devel.* 2010, 13, 527–537.
49. Bauer-Mehren, A.; Furlong, L.I.; Rautschka, M.; Sanz, F. From SNPs to Pathways: Integration of Functional Effect of Sequence Variations on Models of Cell Signalling Pathways. *BMC Bioinform.* 2009, 10 (Suppl. S6).
50. Vanunu, O.; Magger, O.; Ruppín, E.; Shlomi, T.; Sharan, R. Associating Genes and Protein Complexes with Disease via Network Propagation. *PLoS Comput. Biol.* 2010, 6, e1000641.
51. Barabasi, A.L.; Gulbahce, N.; Loscalzo, J. Network Medicine: A Network-Based Approach to Human Disease. *Nat. Rev. Genet.* 2011, 12, 56–68.
52. Akhavan, S.; Miteva, M.A.; Villoutreix, B.O.; Venisse, L.; Peyvandi, F.; Mannucci, P.M.; Guillin, M.C.; Bezaud, A. A Critical Role for Gly25 in the B Chain of Human Thrombin. *J. Thromb. Haemost. JTH* 2005, 3, 139–145.
53. Gallione, C.; Aylsworth, A.S.; Beis, J.; Berk, T.; Bernhardt, B.; Clark, R.D.; Clericuzio, C.; Danesino, C.; Drautz, J.; Fahl, J.; et al. Overlapping Spectra of SMAD4 Mutations in Juvenile Polyposis (JP) and JP-HHT Syndrome. *Am. J. Med. Genet. A* 2010, 152A, 333–339.
54. Sayed, M.G.; Ahmed, A.F.; Ringold, J.R.; Anderson, M.E.; Bair, J.L.; Mitros, F.A.; Lynch, H.T.; Tinley, S.T.; Petersen, G.M.; Giardiello, F.M.; et al. Germline SMAD4 or BMPR1A Mutations and Phenotype of Juvenile Polyposis. *Ann. Surg. Oncol.* 2002, 9, 901–906.
55. Jung, B.; Staudacher, J.J.; Beauchamp, D. Transforming Growth Factor β Superfamily Signaling in Development of Colorectal Cancer. *Gastroenterology* 2017, 152, 36–52.
56. Massagué, J. TGFbeta in Cancer. *Cell* 2008, 134, 215–230.
57. Lori, L.; Pasquo, A.; Lori, C.; Petrosino, M.; Chiaraluce, R.; Tallant, C.; Knapp, S.; Consalvi, V. Effect of BET Missense Mutations on Bromodomain Function, Inhibitor Binding and Stability. *PLoS ONE* 2016, 11, e0159180.
58. Stevanin, G.; Hahn, V.; Lohmann, E.; Bouslam, N.; Gouttard, M.; Soumphonphakdy, C.; Welter, M.-L.; Ollagnon-Roman, E.; Lemainque, A.; Ruberg, M.; et al. Mutation in the Catalytic Domain of Protein Kinase C Gamma and Extension of the Phenotype Associated with Spinocerebellar Ataxia Type 14. *Arch. Neurol.* 2004, 61, 1242–1248.

59. Dehal, P.; Satou, Y.; Campbell, R.K.; Chapman, J.; Degnan, B.; De Tomaso, A.; Davidson, B.; Di Gregorio, A.; Gelpke, M.; Goodstein, D.M.; et al. The Draft Genome of *Ciona intestinalis*: Insights into Chordate and Vertebrate Origins. *Science* 2002, 298, 2157–2167.
60. Takamiya, O.; Seta, M.; Tanaka, K.; Ishida, F. Human Factor VII Deficiency Caused by S339C Mutation Located Adjacent to the Specificity Pocket of the Catalytic Domain. *Clin. Lab. Haematol.* 2002, 24, 233–238.
61. Zhang, Z.; Teng, S.; Wang, L.; Schwartz, C.E.; Alexov, E. Computational Analysis of Missense Mutations Causing Snyder-Robinson Syndrome. *Hum. Mutat.* 2010, 31, 1043–1049.
62. Zhang, Z.; Norris, J.; Schwartz, C.; Alexov, E. In Silico and in Vitro Investigations of the Mutability of Disease-Causing Missense Mutation Sites in Spermine Synthase. *PLoS ONE* 2011, 6, e20373.
63. Wang, Z.; Shen, D.; Parsons, D.W.; Bardelli, A.; Sager, J.; Szabo, S.; Ptak, J.; Silliman, N.; Peters, B.A.; van der Heijden, M.S.; et al. Mutational Analysis of the Tyrosine Phosphatome in Colorectal Cancers. *Science* 2004, 304, 1164–1166.
64. Compiani, M.; Capriotti, E. Computational and Theoretical Methods for Protein Folding. *Biochemistry* 2013, 52, 8601–8624.
65. Marabotti, A.; Scafuri, B.; Facchiano, A. Predicting the Stability of Mutant Proteins by Computational Approaches: An Overview. *Brief. Bioinform.* 2020, 1–17.
66. Kumar, M.D.; Bava, K.A.; Gromiha, M.M.; Prabakaran, P.; Kitajima, K.; Uedaira, H.; Sarai, A. ProTherm and ProNIT: Thermodynamic Databases for Proteins and Protein-Nucleic Acid Interactions. *Nucleic Acids Res.* 2006, 34, D204–D206.
67. Sanavia, T.; Birolo, G.; Montanucci, L.; Turina, P.; Capriotti, E.; Fariselli, P. Limitations and Challenges in Protein Stability Prediction upon Genome Variations: Towards Future Applications in Precision Medicine. *Comput. Struct. Biotechnol. J.* 2020, 18, 1968–1979.
68. Fernald, G.H.; Capriotti, E.; Daneshjou, R.; Karczewski, K.J.; Altman, R.B. Bioinformatics Challenges for Personalized Medicine. *Bioinformatics* 2011, 27, 1741–1748.
69. Niroula, A.; Vihinen, M. Variation Interpretation Predictors: Principles, Types, Performance, and Choice. *Hum. Mutat.* 2016, 37, 579–597.
70. Capriotti, E.; Ozturk, K.; Carter, H. Integrating Molecular Networks with Genetic Variant Interpretation for Precision Medicine. *Wiley Interdiscip. Rev. Syst. Biol. Med.* 2019, 11, e1443.
71. Schymkowitz, J.; Borg, J.; Stricher, F.; Nys, R.; Rousseau, F.; Serrano, L. The FoldX Web Server: An Online Force Field. *Nucleic Acids Res.* 2005, 33, W382–W388.
72. Capriotti, E.; Altman, R.B.; Bromberg, Y. Collective Judgment Predicts Disease-Associated Single Nucleotide Variants. *BMC Genom.* 2013, 14 (Suppl. S3), S2.
73. Capriotti, E.; Calabrese, R.; Casadio, R. Predicting the Insurgence of Human Genetic Diseases Associated to Single Point Protein Mutations with Support Vector Machines and Evolutionary Information. *Bioinformatics* 2006, 22, 2729–2734.
74. Thomas, P.D.; Kejariwal, A. Coding Single-Nucleotide Polymorphisms Associated with Complex vs. Mendelian Disease: Evolutionary Evidence for Differences in Molecular Effects. *Proc. Natl. Acad. Sci. USA* 2004, 101, 15398–15403.
75. Sim, N.-L.; Kumar, P.; Hu, J.; Henikoff, S.; Schneider, G.; Ng, P.C. SIFT Web Server: Predicting Effects of Amino Acid Substitutions on Proteins. *Nucleic Acids Res.* 2012, 40, W452–W457.
76. Bromberg, Y.; Rost, B. SNAP: Predict Effect of Non-Synonymous Polymorphisms on Function. *Nucleic Acids Res.* 2007, 35, 3823–3835.
77. Tate, J.G.; Bamford, S.; Jubb, H.C.; Sondka, Z.; Beare, D.M.; Bindal, N.; Boutselakis, H.; Cole, C.G.; Creatore, C.; Dawson, E.; et al. COSMIC: The Catalogue Of Somatic Mutations In Cancer. *Nucleic Acids Res.* 2019, 47, D941–D947.
78. Kabsch, W.; Sander, C. Dictionary of Protein Secondary Structure: Pattern Recognition of Hydrogen-Bonded and Geometrical Features. *Biopolymers* 1983, 22, 2577–2637.
79. Baugh, E.H.; Ke, H.; Levine, A.J.; Bonneau, R.A.; Chan, C.S. Why Are There Hotspot Mutations in the TP53 Gene in Human Cancers? *Cell Death Differ.* 2018, 25, 154–160.
80. Kim, M.P.; Lozano, G. Mutant P53 Partners in Crime. *Cell Death Differ.* 2018, 25, 161–168.